

## MARIALITE: RIETVELD STRUCTURE-REFINEMENT AND $^{29}\text{Si}$ MAS AND $^{27}\text{Al}$ SATELLITE TRANSITION NMR SPECTROSCOPY

ELENA V. SOKOLOVA<sup>1</sup> AND YURI K. KABALOV

*Department of Crystallography, Faculty of Geology, Moscow State University, Moscow 119899, Russia*

BARBARA L. SHERRIFF AND DAVID K. TEERTSTRA

*Department of Geological Sciences, University of Manitoba, Winnipeg, Manitoba R3T 2N2*

DAVID M. JENKINS

*Department of Geological Sciences and Environmental Studies, Binghamton University, Binghamton, New York 13902-6000, U.S.A.*

GERALD KUNATH-FANDREI, STEFFEN GOETZ AND CHRISTIAN JÄGER

*Institut für Optik und Quantenelektronik, Friedrich-Schiller-Universität, Max-Wien Platz 1, D-07743 Jena, Germany*

### ABSTRACT

The crystal structure of synthetic end-member marialite (Ma)  $\text{Na}_4\text{Al}_3\text{Si}_9\text{O}_{24}\text{Cl}$  and three samples of Na,Cl-rich scapolite from Pamir (central Asia) were refined using Rietveld methods. Compositional measurements indicate meionite (Me)  $\text{Ca}_4\text{Al}_6\text{Si}_6\text{O}_{24}\text{CO}_3$  contents of 0 (SYN MAR), 4.6 (PAM-1), 7.5 (PAM-2), and 7.6% (PAM-3). The crystal structures were refined in space group *I4/m* using ionized X-ray scattering factors:  $R_p$  4.89 – 5.92%,  $R_{wp}$  6.78 – 7.28%,  $R_B$  2.53 – 3.40%,  $R_F$  2.49 – 3.34%,  $s$  1.26 – 2.09. The synthetic end-member marialite has unit-cell parameters  $a = 12.0396(2)$  Å,  $c = 7.5427(2)$  Å and  $V = 1093.3(4)$  Å<sup>3</sup>. A linear correlation was found between the  $a$  and  $c$  unit-cell dimensions and the Si content of these samples of marialitic scapolite. Additional electron-density maxima were found on the difference Fourier maps  $D(xyz)$ , and correlation with an increase with  $\text{H}_2\text{O}$  content suggests partial occupancy by  $\text{H}_2\text{O}$  along the channels of the marialite framework.  $^{27}\text{Al}$  satellite transition NMR spectra show that Al is in only one environment in the natural samples, and  $^{29}\text{Si}$  MAS NMR spectra show that Si alone occupies the  $T1$  site. Calculation of the numbers of Al–O–Si bonds from peak fitting to the  $^{29}\text{Si}$  NMR spectra indicate that up to 80% of the Al atoms in the  $T2$  site are involved in one Al–O–Al bond.

**Keywords:** scapolite, marialite, volatiles, synthesis, Rietveld refinement, XRD, satellite transition NMR, MAS NMR.

### SOMMAIRE

Nous avons affiné la structure cristalline de la marialite synthétique (composition idéal:  $\text{Na}_4\text{Al}_3\text{Si}_9\text{O}_{24}\text{Cl}$ ) et de trois échantillons de scapolite proches de ce pôle, provenant des montagnes Pamir, en Asie centrale, par méthodes de Rietveld. La composition de ces quatre échantillons, en termes de leur teneur en  $\text{Ca}_4\text{Al}_6\text{Si}_6\text{O}_{24}\text{CO}_3$ , est 0 (SYN MAR), 4.6 (PAM-1), 7.5 (PAM-2), and 7.6% (PAM-3). Leur structure a été affinée dans le groupe spatial *I4/m* en utilisant des facteurs de dispersion des rayons X appropriés aux espèces ionisées:  $R_p$  4.89 – 5.92%,  $R_{wp}$  6.78 – 7.28%,  $R_B$  2.53 – 3.40%,  $R_F$  2.49 – 3.34%,  $s$  1.26 – 2.09. Le pôle marialite synthétique possède les paramètres réticulaires suivants:  $a$  12.0396(2) Å,  $c$  7.5427(2) Å,  $V$  1093.3(4) Å<sup>3</sup>. Une relation linéaire existe entre les dimensions  $a$  et  $c$  et le contenu de Si. Des maxima en densité d'électrons ont été documentés sur des cartes de différence Fourier  $D(xyz)$ ; ceux-ci montrent une corrélation avec la teneur en  $\text{H}_2\text{O}$ , ce qui semble indiquer une occupation partielle des canaux dans la trame par des molécules de  $\text{H}_2\text{O}$ . Les spectres de résonance magnétique nucléaire (RMN) des satellites associés à la transition des atomes  $^{27}\text{Al}$  montrent que l'aluminium se trouve dans une seule position dans les échantillons naturels. Les spectres RMN obtenus par spin du  $^{29}\text{Si}$  à angle magique montrent que seul le Si occupe la position  $T(1)$ . Un calcul de la proportion de liaisons Al–O–Si par interprétation des pics à la lumière des spectres RMN de  $^{29}\text{Si}$  indique qu'un maximum de 80% des atomes Al occupant la position  $T2$  seraient impliqués dans une liaison Al–O–Al.

(Traduit par la Rédaction)

**Mots-clés:** scapolite, marialite, phase volatile, synthèse, affinement par méthode de Rietveld, diffraction X, transition des satellites, résonance magnétique nucléaire, spin à angle magique.

<sup>1</sup>E-mail address: evsok@geol.msu.ru

## INTRODUCTION

Scapolite-group minerals have a general formula  $M_4T_{12}O_{24}A$ , and constitute a solid-solution series between the idealized end-members  $Na_4Al_3Si_9O_{24}Cl$  (marialite, Ma) and  $Ca_4Al_6Si_6O_{24}CO_3$  (meionite, Me). Scapolites have three main forms of isomorphous substitution:  $Si^{4+}$  for  $Al^{3+}$  in the *T* site,  $Na^+$  for  $Ca^{2+}$  in the *M* site,  $Cl^-$  for  $CO_3^{2-}$  or  $SO_4^{2-}$  in the *A* site. There can also be minor or trace amounts of K, Sr, Ba and Fe, but only trace quantities of Mg, Mn, Ti, P, Br and F have been measured. Two changes in compositional and cell-parameter trends, at cation contents of  $Na_{3.4}Ca_{0.6}Al_{3.6}Si_{8.4}$  (Me<sub>15</sub>) and  $Na_{1.4}Ca_{2.6}Al_{4.7}Si_{7.3}$  (Me<sub>65</sub>) divide the series into three portions (Teertstra & Sherriff 1996a, Zolotarev 1993). The Me < 15 portion is the focus of this study.

The role of volatile species, including  $H_2O$ , within the scapolite structure is not understood. There are few recent measurements of volatile contents, because H and C can not be measured using the electron-microprobe technique. Also, it is extremely challenging to find the position of these light atoms by refinements of the structure using X-ray-diffraction (XRD) data. Although XRD data do not indicate where the H atoms are situated, infrared (IR) spectroscopic data indicate the presence of abundant bicarbonate and bisulfate (Swayze & Clarke 1990), and Raman spectra suggest the presence of HCl (Donnay *et al.* 1978). Formula calculations have indicated an anion sum for

the *A* site of greater than 1.0 atom per formula unit (apfu), if  $H_2O$  is included with  $Cl^-$ ,  $CO_3^{2-}$  and  $SO_4^{2-}$  (Teertstra & Sherriff 1996b). The natural samples used in this study were analyzed for  $H_2O$ , and intensity peaks found on difference-Fourier maps from powder XRD data are used to investigate the position of the volatile species.

In this study, Rietveld structural refinements of a synthetic sample of end-member marialite and of three samples of marialite with meionite contents of less than 8% enable us to examine trends in the cell parameters for the marialitic portion of the scapolite solid-solution series. Difference-Fourier maps are examined for additional density that would shed light on the position of volatiles in scapolites. We studied the degree of Si–Al order in the tetrahedral sites with MAS and satellite transition NMR spectroscopy.

## REVIEW OF THE STRUCTURAL ANALYSES

Viewed along the *c* axis, the tetrahedral sites in scapolite form two types of 4-membered rings. One ring consists of *T1* tetrahedra that have their apices pointing in the same direction along the *c* axis. In the other ring, the apices of the tetrahedra point alternatively in opposite directions along the *c* axis. In the space group *I4/m*, with a 4-fold rotation axis and a center of inversion, the latter tetrahedra are symmetrically equivalent, so are labeled *T2* (Fig. 1), but in the space group *P4<sub>2</sub>/n*, these become *T2* and *T3*. Viewed along

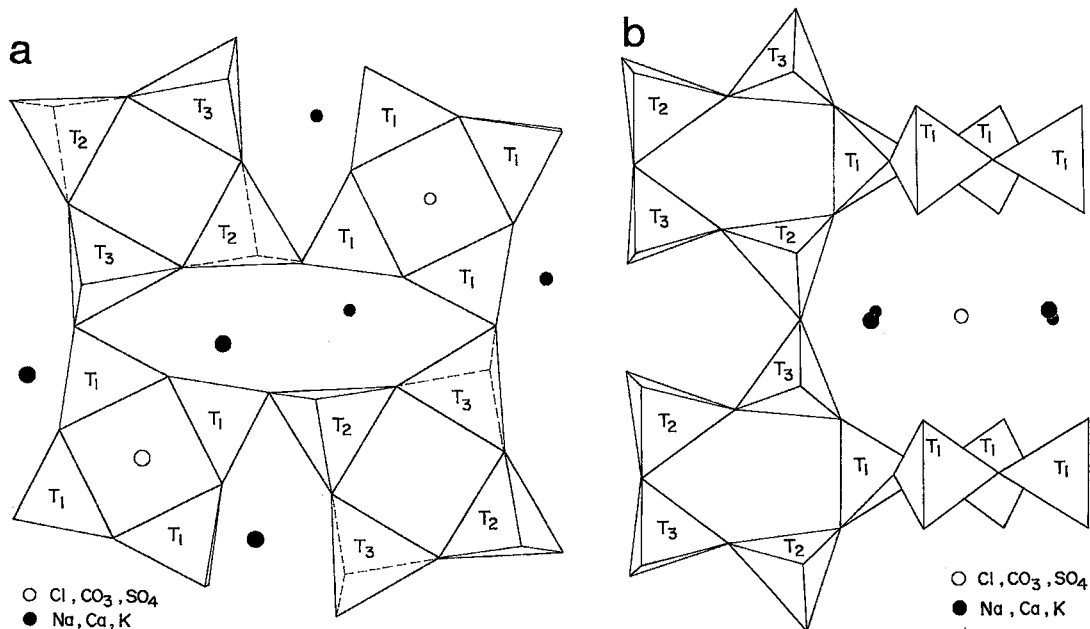


FIG. 1. Crystal structure of scapolite viewed (a) along the *c* axis and (b) along the *a* axis. The *T2* and *T3* sites are equivalent in space group *I4/m*.

the *a* axis, these rings join to form 5-membered rings and large cavities, which each enclose one A anion surrounded by four alkali (*M*) cations. In the present study, the composition of the samples of marialite will be quoted by their meionite content [%Me = 100  $\Sigma$  divalent cations/4], and also by the Si contents (*apfu*).

Teertstra & Sherriff (1996a) showed that variations in the *a* and *V* cell parameters correlate with Si:Al ratio rather than with substitutions in the *M* or *A* site. There is little overall variation of the *c* cell edge with composition across the series. Cell volumes ( $V = a^2c$ ) seem to be constant over the range 0–15% Me, because with decreasing Si content, a decrease in *a* is matched by a slight increase in *c*.

There has been one complete refinement of the structure of a sample with a meionite content of less than 15% or Si greater than 8.4 *apfu* (Si: 8.71 *apfu*; Belokoneva *et al.* 1993); partial data were reported by Comodi *et al.* (1990) for a sample with Si = 8.47 *apfu*. Single-crystal X-ray refinements of the structure show that intermediate members of the series obey space group  $P4_2/n$ , and that the end-members obey  $I4/m$  (Belokoneva *et al.* 1991, 1993, Comodi *et al.* 1990, Papike & Zoltai 1965, Lin & Burley 1973a, b, 1975, Levien & Papike 1976, Papike & Stephenson 1966, Aitken *et al.* 1984, Ulbrich 1973a, b). In this study, structural refinements derived from powder XRD data, by the absence of the weak reflections violating body-centered symmetry, confirm that the space group  $I4/m$  is correct for the long-range symmetry of marialite. The *T*<sub>2</sub> and *T*<sub>3</sub> sites in the space group  $P4_2/n$  become symmetrically equivalent in  $I4/m$ , leading previous investigators to suggest that, in contrast to mid-series scapolites, both end members of the scapolite series have a high degree of Al–Si disorder. The changes of symmetry occur near Me<sub>15</sub> and Me<sub>65</sub> (Teertstra & Sherriff 1996a). It should be emphasized that in compositions with Me < 40%, Al–Si disorder is restricted to the *T*<sub>2</sub> site, as the *T*<sub>1</sub> site is occupied predominantly by Si. XRD observations are consistent with a long-range average structural model. On a unit-cell scale, transmission electron microscopy (TEM) observations suggest lower symmetry and Cl<sup>−</sup> and CO<sub>3</sub><sup>2−</sup> order (Hassan & Buseck 1988).

Magic angle spinning nuclear magnetic resonance (MAS NMR) spectroscopy has been used to investigate the degree of order of Si and Al in the tetrahedral sites, as it provides a short-range view of the structure (Sherriff *et al.* 1987), but in that investigation, owing to the lack of Na- and Cl-rich samples, models of Al–Si order had to be extrapolated to the marialite end-member. Also, there was a problem with quadrupolar interactions causing broad unresolvable peaks in the <sup>27</sup>Al spectra. In this study, this problem is solved by using a combined analysis of the central transition and spinning sidebands of the  $\pm 1/2 \rightleftharpoons \pm 3/2$  satellite transitions, including their envelopes, to investigate

the Al sites. Least-squares fitting of the peaks in the <sup>29</sup>Si spectra gives the proportions of Si in different environments and allows the degree of Si and Al order among the tetrahedral sites to be studied.

## EXPERIMENTAL PROCEDURES

### Materials

The natural samples of scapolite are from the Kukurt hydrothermal scapolite deposit of the Muzcol'sk alpine metamorphic complex in the Eastern Pamir mountain belt in Russia. This Paleozoic gneiss complex has experienced amphibolite-grade metamorphism at the core of an anticline, and amphibolite- and greenschist-grade metamorphism on the flanks. Scapolite is widespread throughout the complex, associated with zones of Na-metasomatism. The Kukurt deposit consists of hydrothermal veins of scapolite with cavities containing transparent crystals of scapolite associated with rutile, ilmenite, titanite and albite. Scapolite also is found in secondary cavities within granitic pegmatites along the Turakuloma mountain ridge (Zolotarev 1993, and references therein). The scapolite crystals in the Kukurt deposit are usually violet, although colorless and yellow crystals also occur. These crystals are usually prismatic, with the dominant forms being {010} and {110}, but {120}, {111}, {221} and {001} may also be present.

Three transparent violet-colored crystals of inclusion-free, gem-quality, marialitic scapolite were selected for study (PAM-1, PAM-2, PAM-3). The euhedral prisms, between 0.5 and 3 cm in length, show a variation in the intensity of the violet color, PAM-2 being the darkest, and PAM-3, the lightest. The crystals were analyzed and checked for homogeneity and purity by powder XRD, electron-microprobe analysis and optical microscopy.

### Synthesis of marialite

Synthetic marialite was produced specifically for NMR spectroscopic studies in a piston-cylinder apparatus from a mixture of reagent grade Na<sub>2</sub>CO<sub>3</sub>, NaCl, Al<sub>2</sub>O<sub>3</sub>, SiO<sub>2</sub>, and Fe<sub>2</sub>O<sub>3</sub>. A preliminary NMR investigation of the marialite synthesized, with the composition Na<sub>4</sub>Al<sub>3</sub>Si<sub>9</sub>O<sub>24</sub>Cl (without Fe), indicated that extremely long *T*<sub>1</sub> relaxation times were needed to acquire the <sup>29</sup>Si spectrum. Accordingly, a mixture was prepared containing 0.1 wt.% Fe<sub>2</sub>O<sub>3</sub> in order to induce a small amount of paramagnetic Fe into the marialite structure to attempt to reduce the *T*<sub>1</sub> relaxation time (*e.g.*, Sherriff & Hartman 1985). If we assume that all of the Fe substitutes for Al as Fe<sup>3+</sup> and that it remained as Fe<sup>3+</sup>, the composition of the resultant marialite would be Na<sub>4.00</sub>Al<sub>2.99</sub>Fe<sub>0.01</sub>Si<sub>9.00</sub>O<sub>24</sub>Cl; unfortunately, this Fe content was not confirmed by EMP analysis (see below).

TABLE 1. MARIALITE: CONDITIONS OF SYNTHESIS

Sample Code	Starting material	T (°C)	P(kbar)	t (h)	Products*
MAR 1-11	Oxide-NaCl mix	1022(10)	17.2(5)	45	Ma, Qtz, Ab
MAR 1-7	Oxide-NaCl mix	1024(10)	16.4(4)	24	Ma, Qtz, Ab(?)
MAR 1-12	MAR 1-11	1033(10)	17.5(3)	72	Ma, [Qtz]
MAR 1-13	MAR 1-7	1033(10)	17.8(3)	92	Ma, [Qtz]
MAR 2-1	Fe-bearing Oxide - NaCl mix	1030(5)	18.6(4)	123	Ma, halite, Qtz
MAR 2-2	Fe-bearing Oxide - NaCl mix	1030(5)	18.8(4)	99	Ma, halite, Qtz
MAR 2-3	MAR 2-1 & 2-2	1032(5)	18.1(4)	194	Ma, halite
MAR 2-4	MAR 2-1 & 2-2	1014(18)	18.3(3)	161	Ma, halite, [Qtz]

\* Abbreviations: Ab; albite, Ma; marialite, Qtz; quartz. Brackets indicate that the phase is present in trace amounts. Uncertainties in last digit are given in parentheses.

The starting mixture was roasted in air at about 1100°C for 30 seconds to drive off CO<sub>2</sub> from the Na<sub>2</sub>CO<sub>3</sub> and to partially fuse the mixture. An additional 15 wt.% NaCl was mixed into the decarbonated starting material in order to ensure that the marialite is saturated in NaCl. Portions of this mixture were sealed (dry) in Pt capsules and treated at 1014–1030°C and 18.1–18.8 kbar for 99–123 hours in a ½-inch piston-cylinder apparatus using solid NaCl pressure media (Johannes 1978). No special attempt was made to control the fugacity of oxygen in the piston-cylinder pressure assemblage.

High but incomplete yields of light blue-grey marialite were obtained from this first treatment, there being minor quartz and albite present along with the excess NaCl. To maximize the yield of marialite, the material obtained from the first treatment was thoroughly ground and treated a second time at the same pressure-temperature conditions for an additional 161–194 hours. This second treatment eliminated all of the albite, and left only a trace (< 1%) of quartz, as judged from the XRD powder pattern. The excess NaCl was rinsed from the sample with distilled water. Examination of the marialite under the petrographic microscope revealed blocky, equant grains 25–30 µm on a side, with low first-order birefringence and a mean index of refraction of 1.536. The conditions for the synthesis of individual runs and also the run products are given in Table 1.

### Chemical analyses

The scapolite crystals were mounted in epoxy resin, polished and then analyzed using a CAMECA SX-50 electron microprobe operating at 15 kV and 20 nA, with a beam diameter 10 µm and count times of 20 s. The data reduction used the PAP procedure (Pouchou & Pichoir 1985). We used, as principal reference standards, gem-quality meionite from Brazil, U.S.N.M. #R6600-1 (Dunn *et al.* 1978), albite from the

Rutherford mine, Amelia Courthouse, Virginia, anorthite from Sitkinak Island, Alaska, and tugtupite from the type locality in southern Greenland (R.O.M. #M32790). Each sample was checked for homogeneity by analysis. Compositions were determined on the same samples from which the X-ray data were measured. The elements Mn, Mg, Ti, P, Br and F were sought, but not detected.

Absolute quantities of H<sub>2</sub>O were determined at 900°C by Karl Fischer titration using a Mitsubishi moisture meter for the three natural samples of marialite. Prior to the determination, the samples were dried at 110°C to remove any water adsorbed on surfaces.

The stoichiometric formulae for the four samples were calculated using the method of Teertstra & Sherriff (1996a, b). This calculation consists of four basic steps: (1) The formula of scapolite is initially calculated by normalizing to Si + Al = 12 *apfu*. Monovalent and divalent cations (including total Fe as Fe<sup>2+</sup>) are assigned to the *M* site. If  $\Sigma M$  is greater than 4 *apfu*, this may indicate that some of the Fe<sup>2+</sup> in *M* should be assigned as Fe<sup>3+</sup> in *T*. The formula can be renormalized to Si + Al + Fe<sup>3+</sup> = 12, generating a lower  $\Sigma M$ . (2) An excess positive charge (*EPC*) is calculated by subtracting the negative charge generated by the framework (*TO*<sub>4</sub><sup>-</sup>) from the positive charge of the *M* cations (*M*<sup>+</sup>) as follows:  $EPC = M^+ - TO_4^- = A^-$ , where  $TO_4^- = Al + Fe^{3+}$ , and  $M^+ = Na + K + 2(Ca + Mg + Sr + Ba + Mn + Fe^{2+})$ . (3) Cl and S contents are usually determined by EMP analysis. By assuming a divalent S species, the remaining anion-charge may be calculated by subtracting Cl, F, and 2S from the *EPC*. The residual charge may be assigned to a divalent charged carbon species, giving a calculated CO<sub>3</sub><sup>2-</sup> *pfu*. (4) If H<sub>2</sub>O is determined and there is a remaining excess positive charge, this may be assigned as OH<sup>-</sup> to balance charges. If there is a net negative charge, this may be assigned as H<sup>+</sup> (*i.e.*, bicarbonate). Any remaining H, when the charges balance, is assigned as molecular H<sub>2</sub>O.

### X-ray powder diffraction

X-ray powder patterns were collected on an ADP-2 diffractometer using CuKα radiation (Ni-filter), a step width of Δ2θ of 0.02°, a 2θ range of 10 to 150° and count times of 5 s per step.

### Rietveld structure refinement

Structure refinements were carried out with the WYRiet, version 3.3 program written by Schneider (1989). The model of Belokoneva *et al.* (1993) for Me<sub>11</sub>, with a space group of *I4/m*, was used as a base for the refinement of the three samples from Pamir. Later, for the sample of synthetic marialite (SYN-MAR), the model for the Me<sub>4,6</sub> (PAM-1) was

used. Two mixing parameters were refined for the pseudo-Voigt profile functions, selected using six full peak-widths at half maximum height (FWHM), and the background was graphically modeled. Refined non-structural parameters included  $2\theta$  zero point, sample displacement, profile parameters  $u$ ,  $v$ , and  $w$ , peak-asymmetry corrections for  $2\theta < 40^\circ$ , and preferred orientation. Scattering factors for ionized species were selected for the refinement of atomic coordinates, isotropic and anisotropic displacement factors. The occupancies of Si were refined at  $T1 = 8(h)$  and  $T2 = 16(i)$ , as were those of Na, and Ca at the  $8(h)$  site. Tables of structure factors are available from the Depository of Unpublished Data, CISTI, National Research Council, Ottawa, Canada K1A 0S2.

For comparative purposes, the structure of the synthetic marialite was refined in the space group  $P4_2/n$  as well as  $I4/m$ . The reflections with  $h + k + l \neq 2n$ , violating the body-centered lattice, would be expected if the structure obeys the space group  $P4_2/n$ .

After refinement, difference-Fourier maps  $D(xyz)$  for the three natural samples indicated additional intensity, which might represent additional positions for volatile species in the structure.

#### Nuclear magnetic resonance spectroscopy

$^{29}\text{Si}$  and  $^{27}\text{Al}$  MAS NMR spectra for the samples PAM-1, PAM-2 and PAM-3 were obtained on a Bruker AMX400 instrument at frequencies of 79.5 and 104.2 MHz, respectively. Rotation rates of 8–14 kHz were obtained using a Bruker high-speed probe.  $^{29}\text{Si}$  spectra were recorded for PAM-1, PAM-2 and PAM-3 with recycle delays of 5 s, as this gave the best signal-to-noise ratio for a given time-period. Spectra recorded for PAM-1 with recycle delays of 1, 5, 30 and 180 s showed differences in relative peak-intensities of less than  $\pm 2\%$  using these differing delays. Relative intensities of the  $^{29}\text{Si}$  peaks were found by simulating the spectra on a computer using a least-squares iterative process, which varied the isotropic chemical shift, the Gaussian and Lorentzian broadening parameters, and the intensity of each line. Short pulses corresponding to tip angles of less than  $\pi/15$  were used for  $^{27}\text{Al}$  in conjunction with a 1 s recycle delay. The baseline roll caused by the finite pulse-length and dead-time was corrected using the cubic spline fit in the spectrometer software (Kunath *et al.* 1992). The spectra were referenced against the  $^{27}\text{Al(VI)}$  resonance of  $\text{Y}_3\text{Al}_5\text{O}_{12}$  at +0.7 ppm. Simulations of the satellite transitions were performed on a 486 processor (Kunath *et al.* 1992) using the theory of Skibsted *et al.* (1991).

$^{29}\text{Si}$  spectra of the two samples of synthetic marialite were obtained at the Prairie Regional NMR Centre on an AMX 500 with a Doty high-speed probe at a frequency of 99.35 MHz. Many attempts were made to

obtain these spectra with different relaxation delays between pulses. The second set of samples was prepared with the addition of Fe to try to increase the relaxation rate. Even with the doped sample the relaxation rate was slow, and the best signal-to-noise ratio was obtained with 148 transients and a 15-minute delay between pulses.

#### RESULTS AND DISCUSSION

Chemical compositions and stoichiometric formulae of the three natural and one synthetic samples of marialite are given in Table 2. The three samples PAM-1, PAM-2 and PAM-3 have compositions  $\text{Me}_{4.6}$ ,  $\text{Me}_{7.5}$  and  $\text{Me}_{7.6}$ , and the Si/Al values are 2.85, 2.72, and 2.71, respectively. It should be noted that PAM-1 and PAM-2 contain more K than PAM-3. Therefore, the low-Me PAM-1 is mainly due to the high values for K and the low levels of Ca rather than the high Na content (Table 2). Samples PAM-1 and PAM-2 have similar  $\text{H}_2\text{O}$  contents, 0.05 and 0.06 wt.%. Although the stoichiometric calculations indicate that this is in the form of  $\text{H}_2\text{O}$  for PAM-1 and  $\text{OH}^-$  for PAM-2 to achieve a balance of charges, there may also be minor  $\text{CO}_3^{2-}$ . PAM-3 has a much higher content with 0.16 wt.%  $\text{H}_2\text{O}$  distributed by charge-balance calculations between 0.08  $\text{OH}^-$  pfu and 0.04  $\text{H}_2\text{O}$  pfu, or 0.08  $\text{H}_2\text{O}$  and 0.04  $\text{CO}_3^{2-}$ .

TABLE 2. CHEMICAL COMPOSITIONS, SAMPLES OF MARIALITE

	SYN-MAR	PAM-1	PAM-2	PAM-3
$\text{SiO}_2$ (wt.%)	64.16	62.53	61.71	61.54
$\text{Al}_2\text{O}_3$	18.01	18.62	19.24	19.31
$\text{Fe}_2\text{O}_3$	0.00	0.07	0.06	0.07
$\text{Na}_2\text{O}$	14.60	12.69	12.36	12.80
$\text{K}_2\text{O}$	0.02	1.57	1.48	0.94
$\text{CaO}$	0.05	1.15	1.92	1.93
$\text{SrO}$	0.00	0.11	0.04	0.14
$\text{BaO}$	0.00	0.00	0.02	0.03
Cl	4.11	4.16	3.93	3.98
$\text{SO}_3$	0.00	0.12	0.15	0.16
$\text{H}_2\text{O}$	n.d.	0.05	0.06	0.16
Sum	100.95	101.00	100.90	100.96
$\text{O}=\text{Cl}_2\text{F}$	-0.92	-0.94	-0.89	-0.80
Total	100.02	100.06	100.01	100.06
Si (apfu)	9.02	8.88	8.78	8.76
Al	2.98	3.12	3.22	3.24
$\text{Fe}^{3+}$	0.00	0.00	0.00	0.01
Na	3.98	3.49	3.41	3.53
K	0.00	0.28	0.27	0.17
Ca	0.01	0.18	0.29	0.29
$\text{Fe}^{2+}$	0.00	0.01	0.01	0.00
Cl	0.98	1.01	0.95	0.96
S	0.00	0.01	0.02	0.02
OH	n.d.	0.00	0.06	0.08
$\text{H}_2\text{O}$	n.d.	0.02	0.00	0.04
Si/Al	3.02	2.85	2.72	2.71
%Me	0.20	4.6	7.5	7.6

The proportions of  $\text{H}_2\text{O}$ , OH,  $\text{Fe}^{2+}$  and  $\text{Fe}^{3+}$  were calculated as described in the text. n.d.: not detected.

TABLE 3. UNIT-CELL PARAMETERS, PATTERN PARAMETERS AND AGREEMENT INDICES FROM RIETVELD REFINEMENT<sup>2</sup>

	SYN-MAR	PAM-1	PAM-2	PAM-3
<i>a</i> (Å)	12.0396(2)	12.047(1)	12.0489(3)	12.0546(2)
<i>c</i> (Å)	7.5427(2)	7.5602(8)	7.5665(2)	7.5684(2)
<i>V</i> (Å <sup>3</sup> )	1093.3(4)	1097.3(2)	1098.47(2)	1099.79(2)
2θ-range(°)	12.0–135.0	12.0–150.0	9.0–124.3	12.0–105.0
Number of reflections	1059	1225	952	692
Number of refined parameters	41	80	80	80
<i>R</i> <sub>p</sub> <sup>2</sup>	5.39	5.92	4.89	5.32
<i>R</i> <sub>wp</sub> <sup>3</sup>	7.04	7.20	6.78	7.28
<i>R</i> <sub>exp</sub> <sup>4</sup>	5.61	4.70	3.49	3.49
<i>R</i> <sub>s</sub> <sup>5</sup>	3.22	3.40	2.86	2.53
<i>R</i> <sub>f</sub> <sup>6</sup>	3.34	3.31	3.22	2.49
<i>s</i> <sup>7</sup>	1.26	1.53	1.94	2.09
DWD <sup>8</sup>	1.38	1.09	0.68	0.72
<i>α</i> <sub>x</sub> <sup>9</sup>	1.730	1.822	2.329	2.272

(1) Refined in space group *I4/m* using X-ray scattering factors for ionized species. (2) *R*<sub>p</sub><sup>2</sup>: pattern *R* factor. (3) *R*<sub>wp</sub>: weighted pattern *R*-factor. (4) *R*<sub>exp</sub>: expected value of *R*<sub>wp</sub>. (5) *R*<sub>s</sub>: Bragg *R*-factor (*R*-value for Bragg intensities). (6) *R*<sub>f</sub>: *R*-value based on the observed and calculated structure-amplitudes. (7) *s* = *R*<sub>wp</sub>/*R*<sub>exp</sub>. (8) DWD: Durbin-Watson statistic (Hill & Flack 1987). (9) *α*<sub>x</sub>: multiplication factor for all values of e.s.d. according to Berar & Lelann (1991).

The refinement results for space groups *P4<sub>2</sub>/n* and *I4/m* were found to be very similar, including interatomic distances for the Al-Si tetrahedra. No reflections with *h* + *k* + *l* ≠ 2*n*, violating the body-centered lattice, were observed by visual inspection of the original X-ray-diffraction pattern or from the calculated residual. Therefore, the higher-symmetry space group *I4/m* was used for all four samples. The refined unit-cell parameters are given in Table 3, atomic coordinates and temperature factors in Table 4, and selected interatomic distances in Table 5.

The values of the cell parameters for synthetic pure end-member marialite (Table 3) are the lowest values recorded so far, and may be used as the reference for end-member marialite. From Table 3, it can be shown that there is a linear trend in *a* and *V* cell parameters from Me<sub>0</sub> to Me<sub>7.6</sub>. *T*-O bond distances can be correlated with the amount of Al in each tetrahedral site. *T*-O bond distances from the Rietveld structural refinement of the three natural samples indicate that the *T*1 site is fully occupied by Si, whereas *T*2 is occupied by both Si and Al (Table 5).

Difference-Fourier maps (00*z*) were calculated with a 0.02 step along the *z* axis to show the position of additional volatile species. The electron-density values

TABLE 4. ATOMIC COORDINATES AND B-FACTORS (Å<sup>2</sup>)

	SYN-MAR	PAM-1	PAM-2	PAM-3
<i>M</i>				
<i>x</i>	0.3741(5)	0.3751(3)	0.3725(9)	0.3729(9)
<i>y</i>	0.2997	0.2981(4)	0.300(1)	0.296(1)
<i>z</i>	0.5	0.5	0.5	0.5
<i>B</i> <sub>1</sub>	4.5(2)	3.63(2)	4.4(3)	3.5(2)
<i>T</i> (1)				
<i>x</i>	0.3386(3)	0.3373(3)	0.3408(9)	0.3372(9)
<i>y</i>	0.4107(2)	0.4109(3)	0.4114(7)	0.4117(7)
<i>z</i>	0	0	0	0
<i>B</i> <sub>1</sub>	1.05(8)	0.71(5)	1.8(2)	0.9(1)
<i>T</i> (2)				
<i>x</i>	0.6611(3)	0.6611(2)	0.6621(5)	0.6611(5)
<i>y</i>	0.9154(3)	0.9151(2)	0.9140(5)	0.9147(5)
<i>z</i>	0.7936(3)	0.7939(3)	0.7936(7)	0.7933(7)
<i>B</i> <sub>1</sub>	1.45(5)	0.53(4)	1.2(1)	0.74(9)
<i>O</i> (1)				
<i>x</i>	0.4564(7)	0.4533(6)	0.457(1)	0.454(1)
<i>y</i>	0.3522(7)	0.3524(5)	0.354(1)	0.355(1)
<i>z</i>	0	0	0	0
<i>B</i> <sub>1</sub>	1.5(3)	1.8(1)	2.5(4)	1.1(4)
<i>O</i> (2)				
<i>x</i>	0.6909(7)	0.6941(6)	0.694(2)	0.692(2)
<i>y</i>	0.8823(7)	0.8801(5)	0.882(8)	0.881(1)
<i>z</i>	0	0	0	0
<i>B</i> <sub>1</sub>	1.5(3)	1.7(2)	1.4(3)	0.9(3)
<i>O</i> (3)				
<i>x</i>	0.3538	0.3518(4)	0.3493(9)	0.3504(9)
<i>y</i>	0.9488	0.9485(4)	0.9501(9)	0.950(1)
<i>z</i>	0.7845(9)	0.7892(7)	0.784(2)	0.786(2)
<i>B</i> <sub>1</sub>	2.0(2)	1.4(1)	2.4(3)	1.6(3)
<i>O</i> (4)				
<i>x</i>	0.2691	0.2718(4)	0.2704(7)	0.2684(9)
<i>y</i>	0.3729	0.3726(3)	0.3741(7)	0.3726(6)
<i>z</i>	0.8250(9)	0.8216(5)	0.826(1)	0.825(1)
<i>B</i> <sub>1</sub>	2.0(2)	1.5(2)	2.4(3)	1.5(3)
<i>Cl</i>				
<i>x</i>	0.5	0.5	0.5	0.5
<i>y</i>	0.5	0.5	0.5	0.5
<i>z</i>	0.5	0.5	0.5	0.5
<i>B</i> <sub>1</sub>	3.8(2)	4.7(5)	7.2(5)	4.9(4)

TABLE 5. SELECTED INTERATOMIC DISTANCES (Å) AND ANGLES (°)

	SYN-MAR	PAM-1	PAM-2	PAM-3
<i>T</i> (1)- <i>O</i> (1)	1.584(5)	1.565(8)	1.555(8)	1.569(9)
<i>T</i> (1)- <i>O</i> (1)'	1.608(5)	1.648(8)	1.601(8)	1.628(8)
<i>T</i> (1)- <i>O</i> (4) × 2	1.628(4)	1.629(5)	1.632(4)	1.635(6)
average	1.612	1.618	1.605	1.617
<i>O</i> (1)- <i>T</i> (1)- <i>O</i> (1)'	110.6(3)	110.4(4)	110.6(4)	108.2(4)
<i>O</i> (1)- <i>T</i> (1)- <i>O</i> (4) × 2	109.6(2)	107.8(3)	110.1(3)	109.3(3)
<i>O</i> (1)- <i>T</i> (1)- <i>O</i> (4)' × 2	109.3(2)	109.6(2)	109.0(3)	110.7(3)
<i>O</i> (4)- <i>T</i> (1)- <i>O</i> (4)'	108.4(2)	111.7(3)	108.0(2)	108.6(3)
average	109.5	109.5	109.5	109.5
<i>T</i> (2)- <i>O</i> (2)	1.647(4)	1.662(3)	1.655(4)	1.658(4)
<i>T</i> (2)- <i>O</i> (3)	1.646(4)	1.651(5)	1.645(5)	1.635(6)
<i>T</i> (2)- <i>O</i> (3)'	1.627(4)	1.649(5)	1.668(5)	1.659(6)
<i>T</i> (2)- <i>O</i> (4)	1.659(4)	1.674(5)	1.637(5)	1.652(5)
average	1.645	1.659	1.656	1.651
<i>O</i> (2)- <i>T</i> (2)- <i>O</i> (3)	107.7(2)	107.2(3)	107.1(3)	107.3(3)
<i>O</i> (2)- <i>T</i> (2)- <i>O</i> (3)'	114.2(2)	115.5(3)	114.3(3)	113.8(4)
<i>O</i> (2)- <i>T</i> (2)- <i>O</i> (4)	105.3(2)	102.8(3)	105.2(3)	105.1(3)
<i>O</i> (3)- <i>T</i> (2)- <i>O</i> (3)'	110.4(2)	112.1(3)	112.5(3)	112.6(3)
<i>O</i> (3)- <i>T</i> (2)- <i>O</i> (4)	111.7(2)	111.6(2)	109.3(2)	110.6(3)
<i>O</i> (3)- <i>T</i> (2)- <i>O</i> (4)'	107.5(2)	107.3(3)	108.1(2)	107.2(3)
average	109.4	109.4	109.4	109.4
<i>M</i> - <i>O</i> 2	2.419(6)	2.394(8)	2.37(1)	2.41(1)
<i>M</i> - <i>O</i> 3 × 2	2.620(5)	2.566(6)	2.600(7)	2.576(7)
<i>M</i> - <i>O</i> 4 × 2	2.896(4)	2.875(5)	2.896(5)	2.910(5)
<i>M</i> - <i>O</i> 4' × 2	3.006(5)	3.030(6)	3.015(6)	2.969(7)
<i>M</i> - <i>Cl</i>	2.848(4)	2.860(5)	2.862(6)	2.893(6)
average	2.789	2.775	2.782	2.777
<i>T</i> (1)- <i>O</i> (1)- <i>T</i> (1)'	159.4(1)	159.6(1)	159.4(1)	161.8(8)
<i>T</i> (2)- <i>O</i> (2)- <i>T</i> (2)'	142.0(1)	139.20(7)	141.40(7)	141.3(3)
<i>T</i> (2)- <i>O</i> (3)- <i>T</i> (2)'	150.7(1)	148.06(9)	149.49(9)	148.9(3)
<i>T</i> (1)- <i>O</i> (4)- <i>T</i> (2)	138.93(8)	136.96(8)	140.28(8)	138.4(3)
average	147.8	146.0	147.6	147.6

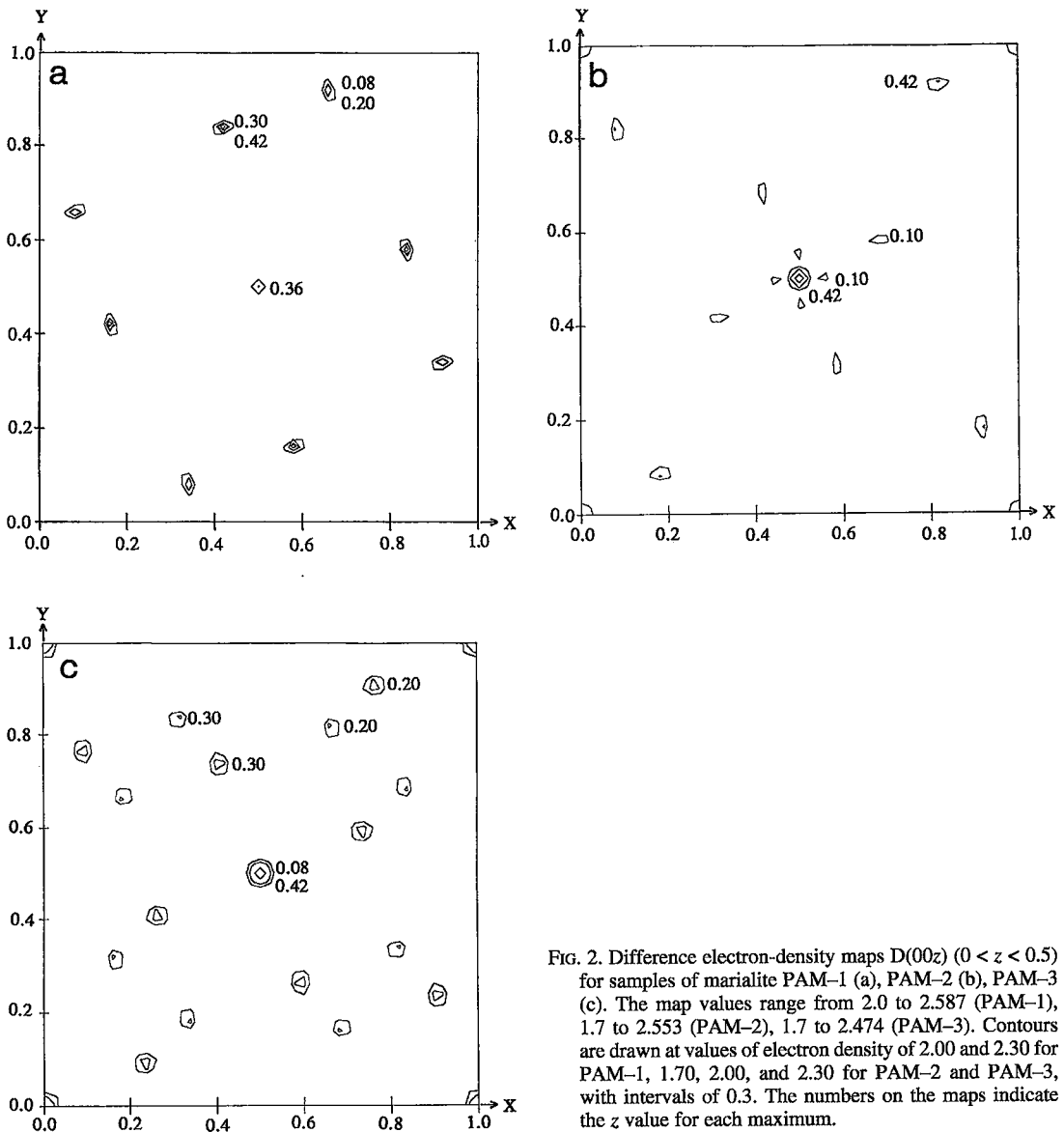


FIG. 2. Difference electron-density maps  $D(00z)$  ( $0 < z < 0.5$ ) for samples of marialite PAM-1 (a), PAM-2 (b), PAM-3 (c). The map values range from 2.0 to 2.587 (PAM-1), 1.7 to 2.553 (PAM-2), 1.7 to 2.474 (PAM-3). Contours are drawn at values of electron density of 2.00 and 2.30 for PAM-1, 1.70, 2.00, and 2.30 for PAM-2 and PAM-3, with intervals of 0.3. The numbers on the maps indicate the  $z$  value for each maximum.

range from 2.0 to 2.587 (PAM-1), 1.7 to 2.553 (PAM-2), 1.7 to 2.474 (PAM-3). Figures 2a, b and c summarize the positions of electron-density maxima for PAM-1, PAM-2 and PAM-3, respectively. To remove background noise and show the projections of the intense maxima only, electron-density contours are drawn at 2.00 and 2.30 for PAM-1, 1.70, 2.00, and 2.30 for PAM-2 and PAM-3, with intervals of 0.3. The numbers on the maps indicate the  $z$  value for each maximum. Comparison of these three figures indicates that there are additional maxima ( $00z$ ) in the large

channels of the structure above and below the A site, which is most pronounced in the  $H_2O$ -rich sample PAM-3. Other maxima, which do not have any specific spatial position but also are situated in the interstices of the structure, occur for all three natural samples. All of the maxima are interpreted as being due to partial occupancy by volatile species, possibly neutrally charged  $H_2O$  molecules. Swayze & Clark (1990) found several different OH-stretching and OH-bending vibrations in their IR spectra of carbonate- and sulfate-rich scapolites. From spectra taken from oriented

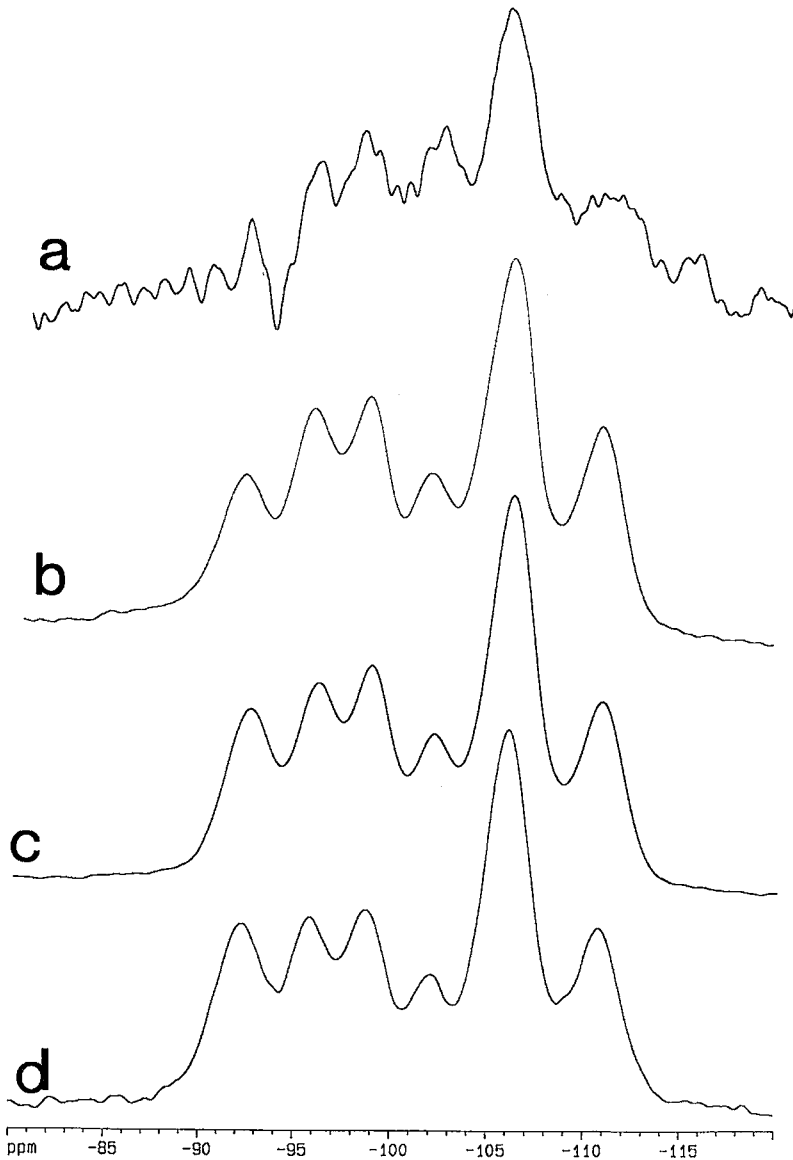


FIG. 3.  $^{29}\text{Si}$  MAS NMR spectra of (a) SYN MAR, (b) PAM-1, (c) PAM-2, and (d) PAM-3.

sections, they determined that the species causing the peaks were in specific crystallographic orientations and not randomly distributed adsorbed water. They concluded that in their samples, OH was related to the carbonate or sulfate group. However, they did not have any samples as Cl-rich as the marialite specimens from Pamir or discuss the possibility of neutral water molecules in the channel above or below the A site. The

additional maxima in our difference-Fourier maps are the first direct information on additional positions for volatile species in the scapolite structure.

The  $^{29}\text{Si}$  MAS NMR spectra of PAM-1, PAM-2 and PAM-3 each consist of six peaks, at  $-92.3$ ,  $-95.8$ ,  $-98.7$ ,  $-102.0$ ,  $-105.8$ ,  $-110.7 \pm 0.1$  ppm (Figs. 3 b, c, d). The relative intensities of the six peaks vary for each spectrum. The relative amounts of the

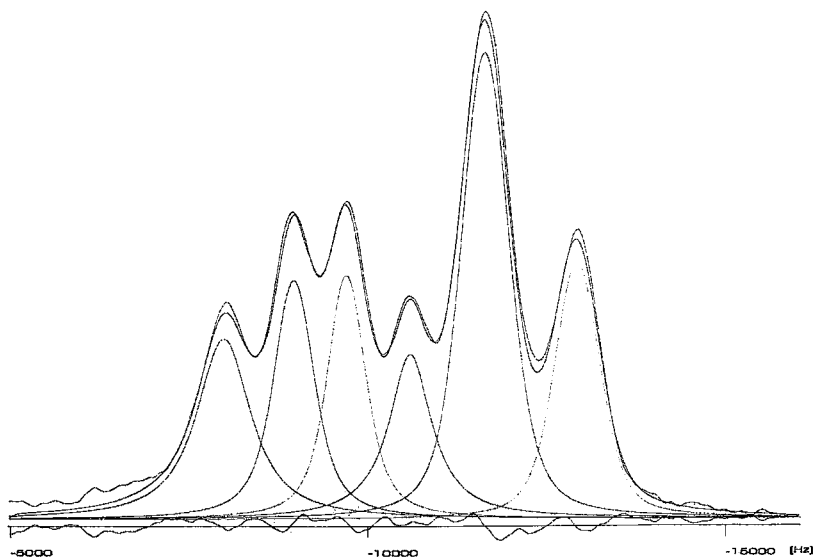


FIG. 4.  $^{29}\text{Si}$  MAS NMR spectrum of PAM-1, with six peaks fitted by the least-squares iterative process; the experimental spectrum, fitted peaks and envelope, and the difference between fitted and experimental spectra are shown.

atoms, in the specific environments relating to each site, were calculated by fitting the spectra to the sums of peaks, which had a combination of Gaussian and Lorentzian line shapes (Fig. 4). The areas under the fitted peaks were converted to relative intensities and related to the number of Si *apfu* contributing to each peak (Table 6). The error on the measurement of relative intensity was found to be  $\pm 2\%$  from the spectra of PAM-1 obtained at differing values of relaxation delays. The  $^{29}\text{Si}$  MAS NMR spectrum of the synthetic marialite had a very poor signal-to-noise ratio (Fig. 3a); however, it can be seen that peaks similar to those of the natural samples are present. The signal-to-noise ratio of this spectrum was considered to be too low to allow a meaningful integration of the peaks or for it to be worth undertaking the laborious fitting procedure on the  $^{27}\text{Al}$  center band and sidebands of satellite transitions.

Previous work has shown that where the Si:Al ratio becomes 2:1, there are only two peaks in the  $^{29}\text{Si}$  spectrum, at  $-92.3$  and  $-105.8$  ppm, due to the two Si environments of  $T3(3\text{Al } 1\text{Si})$  and  $T1(1\text{Al } 3\text{Si})$  (Sherriff *et al.* 1987). Allowing for a shift of about 4 ppm to high field for each substitution of a neighboring Al for Si, the six peaks in the  $^{29}\text{Si}$  spectra of the marialite samples at  $-92.3$ ,  $-95.8$ ,  $-98.7$ ,  $-102.0$ ,  $-105.8$ ,  $-110.7$  ppm were allocated to  $T2(1\text{Si}3\text{Al})$ ,  $T2(2\text{Si}2\text{Al})$ ,  $T2(3\text{Si}1\text{Al})$ ,  $T2(4\text{Si})$ ,  $T1(3\text{Si}1\text{Al})$  and  $T1(4\text{Si})$ , respectively.

As Al increases from 3.12 to 3.24 *apfu* from PAM-1 to PAM-3, there is an increase in the intensity of the  $T2(1\text{Si}3\text{Al})$  and  $T1(3\text{Si}1\text{Al})$  peaks, at  $-92.3$  and  $-105.8$  ppm, relative to the peaks due to  $T2(2\text{Si}2\text{Al})$ ,  $T2(3\text{Si}1\text{Al})$ ,  $T2(4\text{Si})$ , and  $T1(4\text{Si})$  sites, as expected (Table 6). There are 4.00 Si *apfu* in the  $T1$  sites for all three samples, within experimental error, corroborating that the single peak in each  $^{27}\text{Al}$  spectrum is due to Al in the  $T2$  site, and that there is no significant amount of Al in the  $T1$  site.

TABLE 6. RELATIVE INTENSITIES FOR  $^{29}\text{Si}$  MAS NMR SPECTRA

Peak position and allocation*	Peak allocation	PAM-1	PAM-2	PAM-3
$-92.3$ ppm	$T2(1\text{Si}3\text{Al})$	16% (1.4)	15% (1.3)	17% (1.5)
$-95.8$ ppm	$T2(2\text{Si}2\text{Al})$	14% (1.3)	14% (1.2)	14% (1.2)
$-98.7$ ppm	$T2(3\text{Si}1\text{Al})$	13% (1.2)	14% (1.2)	13% (1.1)
$-102.0$ ppm	$T2(4\text{Si})$	12% (1.0)	12% (1.1)	11% (1.0)
Total for $T2$		55% (4.9)	55% (4.8)	55% (4.8)
$-105.8$ ppm	$T1(3\text{Si}1\text{Al})$	30% (2.6)	30% (2.7)	30% (2.7)
$-110.7$ ppm	$T1(4\text{Si})$	15% (1.4)	15% (1.3)	15% (1.3)
Total for $T1$		45% (4.0)	45% (4.0)	45% (4.0)
Total		100% (8.9)	100% (8.8)	100% (8.8)

number of Si atoms per formula unit in parentheses.

\*T refers to tetrahedral sites containing either Si or Al.

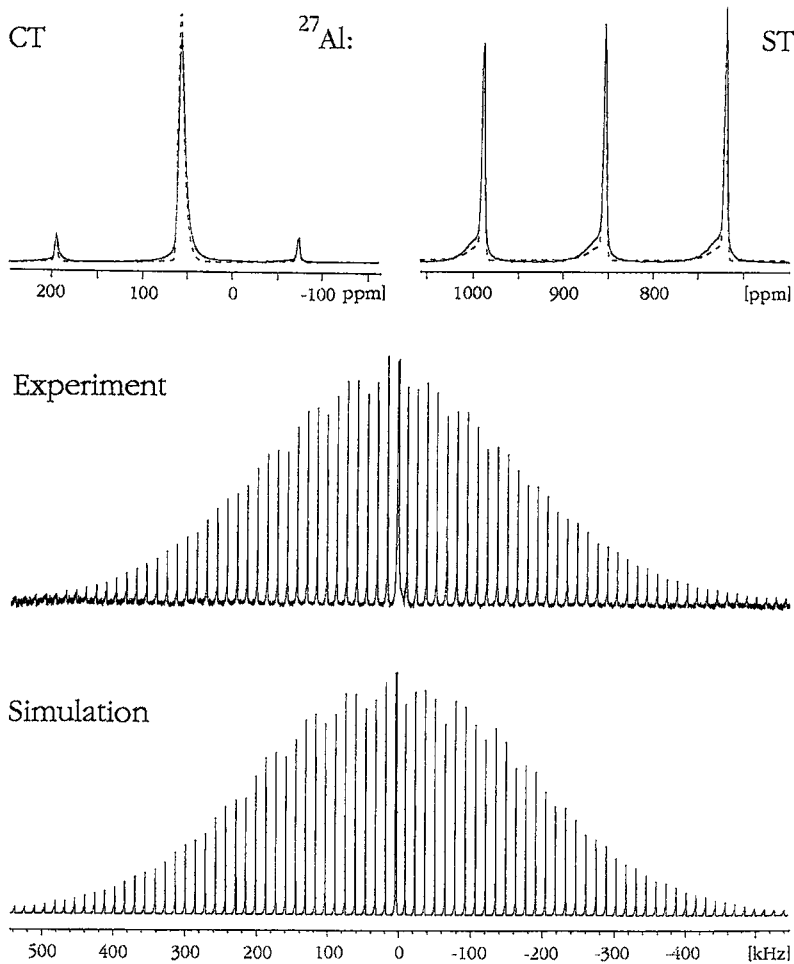


FIG. 5.  $^{27}\text{Al}$  satellite transition spectra of PAM-1 showing the experimental (solid line) and fitted (dashed line) central transition (CT) and satellite transition (ST) line-shape, and the experimental and simulated sideband envelope.

The  $^{27}\text{Al}$  spectra for the three natural samples have a similar single center band and satellite transition sideband peaks. The isotropic chemical shift of 58.7 ppm, quadrupolar coupling constant  $C_Q$  of 1.98 MHz and asymmetry parameter  $\eta$  of 0.8 to 1.0 were calculated by fitting the shape of the center band and sideband and the sideband envelope (Fig. 5) using 350 Hz Gaussian line broadening. Al appears to be in a single  $T_2$  environment in the three samples, in agreement with the  $T$ -O bond distances calculated from the Rietveld refinements and with the  $^{29}\text{Si}$  MAS NMR spectra. However, there is a distribution in the quadrupolar coupling constant of 85 kHz, indicating some slight variation in environment among Al sites.

It would be expected from the Al avoidance rule (Lowenstein 1954) that where Al is sufficiently dilute in the system, there will be no Al-O-Al bonds. Therefore, only (4Si) sites should be present in these compositions of scapolite. However, if the total number of Al atoms is calculated from the relative intensities of the peaks fitted to each  $^{29}\text{Si}$  spectrum using the formula:

$$\text{Al} = \sum_{m=0}^4 (m/4) I_{4,m}$$

[Engelhardt & Michel (1987) and references therein], the results for PAM-1, PAM-2 and PAM-3 are 2.6, 2.6 and 2.7, respectively, instead of the expected values of 3.1, 3.2, and 3.2. This translates into 3.4, 3.2 and

3.3 Al–O–Si bonds per Al atom instead of the 4 that would be expected. Either there is less Al in the unit cell than has been calculated from the electron-microprobe analyses, or up to 80% of the Al atoms are involved in one Al–O–Al bond, in violation of Lowenstein's rule.

Tossell (1993) calculated that the difference in energy between paired and alternating Si and Al atoms in a four-membered ring of  $\text{Si}_2\text{Al}_2\text{O}_{12}\text{H}_8^{2-}$  is only 63 kJ/mol rather than the previously calculated values of >400 kJ/mol (Hass *et al.* 1981, Sauer & Engelhardt 1982, Navrotsky *et al.* 1985, Derouane *et al.* 1990, Pelmenschikov *et al.* 1992). This value is further reduced by about 22 kJ/mol by the addition of a single Na cation to the atom of bridging oxygen, as is present in the structure of marialitic scapolite. This 40 kJ/mol result is consistent with the calorimetric data of Navrotsky *et al.* (1982, 1985) and the study of lattice-energy minimization (Bell *et al.* 1992). With these small differences in energy, either of the two configurations is possible. Therefore, we suggest that the single  $^{27}\text{Al}$  peak in the marialite samples originates from the T2(3Si1Al) environment. The lack of a small  $^{27}\text{Al}$  peak expected from the T1(4Si) may be due to the lack of resolution of the (4Si) and (1Al3Si) peaks under the broad center and sideband peaks, but also may be the cause of the distribution of the quadrupolar coupling constant.

At this point, there is no evidence as to whether the Al–O–Al bonds are within or between the 4-membered T2 rings. The distance from Na to O(4), between the 4-membered rings, is 2.9 to 3.0 Å, whereas within the 4-membered rings, the distance from Na to O(2) is 2.4 Å, and to O(3), it is 2.6 Å. Therefore, the stabilizing influence would be greater within the four-membered rings, where the Na–O bond is the shortest. We interpret these data to indicate that there are Al–O–Al bonds within the four-membered T2 rings.

#### CONCLUSIONS

1. Rietveld refinement from X-ray powder data of the marialite samples from the Pamir Mountains confirm tetragonal symmetry described by space group  $I4/m$ . There is a linear trend in the cell parameters for the synthetic marialite end-member through the natural samples ( $\text{Me}_{4.6}$ ,  $\text{Me}_{7.5}$  and  $\text{Me}_{7.6}$ ).
2. Our structural refinement of  $\text{Me}_{4.6}$  (PAM-1) is the closest so far to the natural marialite end-member. The synthetic Ma end-member has unit-cell parameters  $a$  12.0396(2) Å,  $c$  7.5427(2) Å, with  $V$  equal to 1093.3(4) Å<sup>3</sup>.
3. Additional electron-density maxima on the difference Fourier maps indicate that there are volatile species, probably neutral H<sub>2</sub>O molecules, in the interstices above and below the A site in the structure of marialite.

4.  $^{27}\text{Al}$  satellite transition and  $^{29}\text{Si}$  MAS NMR spectra show that Al is located only in the T2 site. There is a strong indication that Al–O–Al bonds are present between most of the Al atoms in these compositions of scapolite, in contravention of Lowenstein's rule, but in agreement with the calculations of Tossell (1993).

#### ACKNOWLEDGEMENTS

Samples were kindly provided by S. Sergeev and F. Rafikova. Research expenses were supported by a Russian Fund for Basic Research grant 95-05-15699 to E.V.S. and Y.K.K., a Natural Sciences and Engineering Research Council University Research Fellowship and Research Grant to B.L.S., and National Science Foundation Grant EAR-9316079 to D.M.J. Special thanks are given to David A. Vanko for advice on the synthesis of marialite. We thank Jian-jie Liang, an anonymous referee and Associate Editor Peter B. Leavens and Robert F. Martin for helpful comments on this manuscript.

#### REFERENCES

- AITKEN, B.G., EVANS, H.T., JR. & KONNERT, J.A. (1984): The crystal structure of a synthetic meionite. *Neues Jahrb. Mineral. Abh.* **149**, 309-342.
- BELL, R.G., JACKSON, R.A. & CATLOW, C.R.A. (1992): Lowenstein's rule in zeolite A: a computational study. *Zeolites* **12**, 870-871.
- BELOKONEVA, E.L., SOKOLOVA, N.V. & DOROKHOVA, G.I. (1991): Crystal structure of natural Na,Ca-scapolite – an intermediate member of the marialite-meionite series. *Sov. Phys. Crystallogr.* **36**, 828-830.
- , ——— & URUSOV, V.S. (1993): Scapolites – crystalline structures of marialite (Me11) and meionite (Me88) – space group as a function of composition. *Crystallogr. Rep.* **38**(1), 25-28 (translated from *Kristallogr.* **38**, 52-77).
- BERAR, J.-F. & LELANN, P. (1991): E.S.D's and estimated probable error obtained in Rietveld refinements with local correlations. *J. Appl. Crystallogr.* **24**, 1-5.
- COMODI, P., MELLINI, M. & ZANAZZI, P.F. (1990): Scapolites: variation of structure with pressure and possible role in the storage of fluids. *Eur. J. Mineral.* **2**, 195-202.
- DEROUANE, E.G., FRIPIAT, J.G. & BALLMOOS, R. (1990): Quantum mechanical calculations on molecular sieves. II. Model cluster investigation of silicoaluminophosphates. *J. Phys. Chem.* **94**, 1687-1692.
- DONNAY, G., SHAW, C.F., III, BUTLER, I.S. & O'NEIL, J.R. (1978): The presence of HCl in scapolites. *Can. Mineral.* **16**, 341-345.
- DUNN, P.J., NELEN, J.E. & NORBERG, J. (1978): On the composition of gem scapolites. *J. Gemmol.* **16**, 4-10.

- ENGELHARDT, G. & MICHEL, D. (1987): *High Resolution Solid State NMR of Silicates and Zeolites*. John Wiley and Sons, New York, N.Y.
- HASS, E.C., MEZEY, P.G. & PLATH, P.J. (1981): A non-empirical molecular orbital study on Lowenstein's rule and zeolite composition. *J. Molecular Struct.* **76**, 389-399.
- HASSAN, I. & BUSECK, P.R. (1988): HRTEM characterization of scapolite solid solutions. *Am. Mineral.* **73**, 119-134.
- HILL, R.G. & FLACK, H.D. (1987): The use of the Durbin-Watson d statistic in Rietveld analysis. *J. Appl. Crystallogr.* **20**, 356-361.
- JOHANNES, W. (1978): Pressure comparing experiments with NaCl, AgCl, talc, and pyrophyllite assemblies in a piston cylinder apparatus. *Neues Jahrb. Mineral., Monatsh.*, 84-92.
- KUNATH, G., LOSSO, P., STEUERNAGEL, S., SCHNEIDER, H. & JÄGER, C. (1992):  $^{27}\text{Al}$  satellite transition spectroscopy (SATRAS) of polycrystalline aluminium borate  $9\text{Al}_2\text{O}_3 \cdot 2\text{B}_2\text{O}_3$ . *Solid State Nuclear Magn. Res.* **1**, 261-266.
- LEVIEN, L. & PAPIKE, J.J. (1976): Scapolite crystal chemistry: aluminum-silicon distributions, carbonate group disorder and thermal expansion. *Am. Mineral.* **61**, 864-877.
- LIN, S.B. & BURLEY, B.J. (1973a): Crystal structure of a sodium and chlorine-rich scapolite. *Acta Crystallogr.* **B29**, 1272-1278.
- & ————— (1973b): On the weak reflections violating body-centered symmetry in scapolites. *Tschermaks Mineral. Petrogr. Mitt.* **20**, 28-44.
- & ————— (1975): The crystal structure of an intermediate scapolite - wernerite. *Acta Crystallogr.* **B31**, 1806-1814.
- LOWENSTEIN, W. (1954): The distribution of aluminum in the tetrahedra of silicates and aluminosilicates. *Am. Mineral.* **39**, 92-96.
- NAVROTSKY, A., GEISINGER, K.L., McMILLAN, P. & GIBBS, G.V. (1985): The tetrahedral framework in glasses and melts: inferences from molecular orbital calculations and implications for structure, thermodynamics and physical properties. *Phys. Chem. Minerals* **11**, 284-298.
- , PERAUDEAU, G., McMILLAN, P. & COUTURES, J.-P. (1982): A thermochemical study of glasses and crystals along the joins silica - calcium aluminate and silica-sodium aluminate. *Geochim. Cosmochim. Acta* **46**, 2039-2047.
- PAPIKE, J.J. & STEPHENSON, N.C. (1966): The crystal structure of mizzonite, a calcium- and carbonate-rich scapolite. *Am. Mineral.* **51**, 1014-1027.
- & ZOLTAI, T. (1965): The crystal structure of a marialite scapolite. *Am. Mineral.* **50**, 641-655.
- PELMENSCHIKOV, A.G., PAUKSHITS, E.A., EDISHERASHVILI, M.O. & ZHDOMIROV, G.M. (1992): On the Lowenstein's rule and mechanism of zeolite dealumination. *J. Phys. Chem.* **96**, 7051-7055.
- POUCHOU, J.L. & PICHOR, F. (1985) "PAP" (phi-rho-Z) procedure for improved quantitative microanalysis. In *Microbeam Analysis* (J.T. Armstrong, ed.). San Francisco Press, San Francisco, California (104-106).
- SAUER, J. & ENGELHARDT, G. (1982): Relative stability of Al-O-Al linkages in zeolites. A non empirical molecular orbital study. *Z. Natur.* **37A**, 277-279.
- SCHNEIDER, J. (1989): Profile refinement on IBM-PC's. *I.U.Cr. Int. Workshop on the Rietveld method*. M. Schneider EDV, Beijing, China.
- SHERRIFF, B.L., GRUNDY, H.D. & HARTMAN, J.S. (1987): Occupancy of T-sites in the scapolite series. A multi-nuclear NMR study using magic angle spinning. *Can. Mineral.* **25**, 717-730.
- & HARTMAN, J.S. (1985): Solid-state high-resolution  $^{29}\text{Si}$  NMR of feldspars: Al-Si disorder and the effects of paramagnetic centers. *Can. Mineral.* **23**, 205-212.
- SKIBSTED, J., NIELSON, N.C., BILDSØE, H. & JAKOBSEN, H.J. (1991): Satellite transitions in MAS NMR spectra of quadrupolar nuclei. *J. Magn. Res.* **95**, 88-117.
- SWAYZE, G.A. & CLARK, R.N. (1990): Infrared spectra and crystal chemistry of scapolites: implication for Martian mineralogy. *J. Geophys. Res.* **95**, 14481-14495.
- TEERTSTRA, D.K. & SHERRIFF, B.L. (1996a): Scapolite cell parameter trends along the solid solution series. *Am. Mineral.* **81**, 169-180.
- & ————— (1996b): Substitutional mechanisms, compositional trends and the end member formulae of scapolite. *Chem. Geol.* (??Jan. 1996)
- TOSSELL, J.A. (1993): A theoretical study of the molecular basis of the Al avoidance rule and of the spectral characteristics of Al-O-Al linkages. *Am. Mineral.* **78**, 911-920.
- ULBRICH, H.H. (1973a): Crystallographic data and refractive indices of scapolites. *Am. Mineral.* **58**, 81-92.
- (1973b): Structural refinement of the Monte Somma scapolite, a 93% meionite. *Schweiz. Mineral. Petrogr. Mitt.* **53**, 385-393.
- ZOLOTAREV, A.A. (1993): Gem scapolite from the eastern Pamirs and some general constitutional features of scapolites. *Zap. Vses. Mineral. Obshchest.* **122**, 90-102.